Phase diagram of the Hubbard-Kondo lattice model from the variational cluster approximation

J. P. L. Faye and M. N. Kiselev

The Abdus Salam International Center for Theoretical Physics, Strada Costiera 11, 34014 Trieste, Italy

P. Ram and B. Kumar

School of Physical Sciences, Jawaharlal Nehru University, New Delhi 110067, India

D. Sénéchal

Département de physique and Institut Quantique, Université de Sherbrooke, Sherbrooke, Québec, Canada J1K 2R1

The interplay between the Kondo effect and magnetic ordering driven by the Ruderman-Kittel-Kasuya-Yosida interaction is studied within the two-dimensional Hubbard-Kondo lattice model. In addition to the antiferromagnetic exchange interaction $J_\perp$ between the localized spins and the conduction electrons, this model also contains the local repulsion U between the conduction electrons. We use variational cluster approximation to investigate the competition between the antiferromagnetic phase, the Kondo singlet phase, and a ferrimagnetic phase on square lattice. At half-filling, the Néel antiferromagnetic phase dominates from small to moderate $J_\perp$ and $U J_\perp$, and the Kondo singlet elsewhere. Sufficiently away from half-filling, the antiferromagnetic phase first gives way to a ferrimagnetic phase (in which the localized spins order ferromagnetically, and the conduction electrons do likewise, but the two mutually align antiferromagnetically), and then to the Kondo singlet phase.

I. INTRODUCTION

The interaction between itinerant electrons and impurity spins plays a key role in many areas of condensed matter physics, including, but not limited to, quantum materials, spintronics, and quantum information processing [1]. In quantum materials, this interaction can arise either through (i) the hybridization of valence electrons with localized d or f orbitals or (ii) a coupling of the electron spin density to the spins of the localized electrons. In the first case, it can be argued that the Kondo exchange [2] becomes the dominant interaction if the localized orbitals, with a weak hybridization, are slightly occupied [3]. In the second case, corresponding to half-filled local orbitals, the Kondo lattice model presents a generic minimal description of the low-energy physics. These two mechanisms describe the physics of two main families of the strongly correlated heavy fermion (HF) systems: In uranium-based HF systems, the $5f$ electrons are strongly hybridized with s, p, or d itinerant electrons. As a result, there exist strong charge (valence) fluctuations. By contrast, the $4f$ level in cerium-based HF systems is located well below the Fermi level, due to which the charge fluctuations are frozen out and the spin fluctuations play the central role. The effective model describing their low-energy physics is known as the Kondo lattice model [2,4–6].

The ground state of the Kondo lattice model at half-filling is insulating either due to the formation of singlets between the local moments and the cloud of conduction electrons (Kondo cloud) [7], or due to magnetic ordering of local moments via the Ruderman-Kittel-Kasuya-Yosida (RKKY) mediated by itinerant electrons [5,8–11]. The mean field theory reveals that the magnetic correlations depend on the density of conduction electrons: they are antiferromagnetic (AFM) near half-filling

and ferromagnetic (FM) at lower fillings [12]. Increasing the exchange interaction between the conduction electrons and the localized moments leads the magnetic system to the spin-gapped Kondo singlet phase. The spin gap formation associated with hidden symmetries has been investigated analytically in spin chains with AFM Heisenberg exchange interactions coupling the conduction and the localized spins [13]. This study was supported by Monte Carlo simulations [14,15]. Notice that these chains called spin-rotor chains are similar to the spiral staircase Heisenberg ladder [16] for the study of Kondo physics.

The Kondo lattice model of noninteracting conduction electrons is the most promising candidate to capture the qualitative physics of the HF systems, but it fails to correctly describe the physics at lower temperature scale [17]. One example is the electron-doped cuprate $Nd_{2-x}Ce_xCuO_4$ [18], wherein it is suggested that the Kondo effect plays some important role due to strong correlation among the charge carriers and therefore cannot be neglected. Indeed, the interaction between conduction electrons can play a crucial role and even enhance the Kondo temperature significantly [17]. In this spirit, some effort has been undertaken to study the influence of correlations of conduction electrons on the Kondo effect both for impurity [19–22] and lattice models [23–26]. A Hubbard-type repulsion U was introduced among the conduction electrons, resulting in the Hubbard-Kondo lattice model. This model was studied at half-filling [25] using dynamical mean field theory [27,28], with an impurity model consisting of two correlated orbitals. In Ref. [29], the role of this Coulomb repulsion was investigated using both $T = 0$ quantum Monte Carlo and a bond-operator mean field theory at half-filling. One of their findings is that this model displays a magnetic order-disorder transition with

a critical Kondo interaction which decreases as a function of the Hubbard repulsion.

In this paper we study the interplay between the Kondo effect and the magnetic ordering within the Hubbard-Kondo lattice model. The model includes a local Coulomb repulsion U between the conduction electrons, in addition to the AFM Kondo interaction $J_\perp$ between the localized spin-1/2 moments and the conduction electrons. We obtain its quantum phase diagram at half-filling, and also at finite dopings, using the variational cluster approximation (VCA) [30–32]. The VCA is an approach based on a rigorous variational principle that treats short-range correlations exactly. At half-filling, we find that the ground state is a Néel AFM at moderate to small values of $J_\perp$ and $U J_\perp$, while the Kondo singlet phase is stable at large $J_\perp$ and U. The transition from the AFM to the Kondo singlet phase is continuous (second order). At finite doping we find that the antiferromagnet survives close to half-filling and disappears upon doping further or increasing U (at least for small U). Then a ferrimagnetic phase becomes stable at lower densities and small exchange interactions. The Kondo singlet appears at large $J_\perp$ for all values of the conduction electron density. The transition from the magnetically ordered to the Kondo singlet phase becomes discontinuous (first order) away from half-filling.

The paper is organized as follows. In Sec. II we define the model and briefly review the VCA method. We present and discuss our results in Sec. III and conclude in Sec. IV.

II. MODEL AND METHOD

The Kondo lattice model (or the necklace Hamiltonian) was introduced by Doniach [16]. It can be formulated as a tight-binding model of the conduction electrons on a lattice, where on each site there also sits a local spin that couples to the conduction electron spin. The Hubbard-Kondo model is obtained by adding to the Kondo lattice model a local Coulomb repulsion U for the conduction electrons.

A. Hubbard-Kondo lattice model

The Hamiltonian of the Hubbard-Kondo lattice model on square lattice can be written as follows:

$$H_{\mathrm{HK}} = -t \sum_{\langle i,j\rangle \sigma} c_{i\sigma}^\dagger c_{j\sigma} - t' \sum_{\langle\langle i,j\rangle\rangle \sigma} c_{i\sigma}^\dagger c_{j\sigma} - \mu \sum_{i\sigma} n_{i\sigma}$$
$$+ U \sum_i n_{i\uparrow} n_{i\downarrow} + J_\perp \sum_i \mathbf{s}_i \cdot \mathbf{S}_i. \qquad (1)$$

In the above equation, $c_{i\sigma}$ annihilates a conduction electron at site i with spin σ, t is the nearest-neighbor and t' is the next-nearest-neighbor hopping amplitude, μ is the chemical potential, and U is the on-site repulsion between the conduction electrons. The number of conduction electrons at site i with spin σ is $n_{i\sigma} = c_{i\sigma}^\dagger c_{i\sigma}$. The $J_\perp$ is the exchange interaction between the itinerant spins $\mathbf{s}_i = \frac{1}{2} \sum_{\sigma,\sigma'} c_{i\sigma}^\dagger \boldsymbol{\tau}_{\sigma\sigma'} c_{i\sigma'}$, and the localized spin-1/2's $\mathbf{S}_i$. We assume an AFM Kondo coupling: $J_\perp > 0$. In this paper we will define all quantities in units of the hopping amplitude t, that is, set $t = 1$. The model (1) neglects explicit hybridization between the local and the conduction electrons, although it implicitly exists through $J_\perp$. This is a

good approximation for Ce-based heavy fermion materials (see details in the review article [33]) in the regime of integer valence where the $4f$ levels are located well below the Fermi level and, therefore, their hybridization with the itinerant d electrons is small.

We employ the VCA method to investigate this model. But our implementation of the VCA can only deal with the fermion operators. Hence, for the localized spins, we use the representation $\mathbf{S}_i = \frac{1}{2} \sum_{\sigma,\sigma'} f_{i\sigma}^\dagger \boldsymbol{\tau}_{\sigma\sigma'} f_{i\sigma'}$ in terms of the electronlike fermion operators $f_{i,\sigma}$ and $f_{i,\sigma}^\dagger$. To ensure that this representation describes a pure localized spin-1/2, we introduce an auxiliary, particle-hole symmetric, local repulsion U_f between the f fermions. When U_f is very large (larger than the parameters of the Hubbard-Kondo lattice model), it guarantees that the f fermions correctly describe the localized spin-1/2 moments. So, in effect, we study

$$H = H_{\mathrm{HK}} + U_f \sum_i \left[n_{i\uparrow}^f n_{i\downarrow}^f - \frac{1}{2} \left(n_{i\uparrow}^f + n_{i\downarrow}^f \right) \right], \qquad (2)$$

using VCA for a fixed large value of $U_f (=100)$.

B. The variational cluster approximation

In order to probe the possibility of magnetism in model (2), we use the variational cluster approximation (VCA) with an exact diagonalization solver at zero temperature [30]. This method has been applied to many strongly correlated systems in connection with various broken symmetry phases, for example in superconductivity [34,35] and magnetism [36]. For a detailed review of the method, see Refs. [31,32]. Like other quantum cluster methods, VCA starts by a tiling of the lattice into an infinite number of identical clusters. We will use the eight-site cluster illustrated in Fig. 1. In VCA, one considers two systems: the original system described by the Hamiltonian H, defined on the infinite lattice, and the *reference system*, governed by the Hamiltonian H', defined on the cluster only, with the same interaction part as H. Typically, H' will be a restriction of H to the cluster (i.e., with intercluster hopping removed), to which various Weiss fields may be added in order
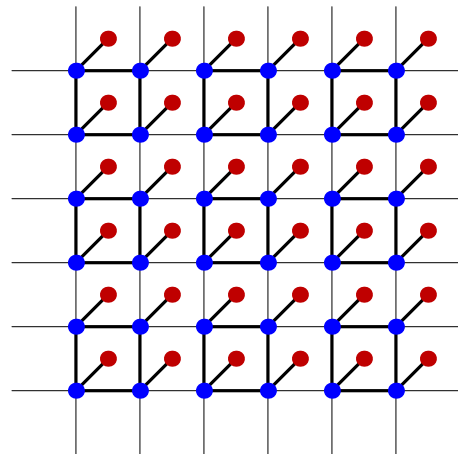
FIG. 1. The Hubbard-Kondo lattice and its decomposition into identical eight-site clusters. The conduction and localized orbitals are represented by blue and red dots, respectively.

to probe broken symmetries. More generally, any one-body term can be added to H'. The size of the cluster should be small enough for the electron Green function to be computed numerically by an exact diagonalization method. The optimal one-body part of H' is determined by a variational principle. More precisely, the electron self-energy $\boldsymbol{\Sigma}$ associated with H' is used as a variational self-energy, in order to construct the Potthoff self-energy functional [37]:

$$\Omega[\boldsymbol{\Sigma}(\xi)] = \Omega'[\boldsymbol{\Sigma}(\xi)] + \mathrm{Tr}\ln\left[-\left(\mathbf{G}_0^{-1} - \boldsymbol{\Sigma}(\xi)\right)^{-1}\right] - \mathrm{Tr}\ln(-\mathbf{G}'(\xi)). \tag{3}$$

The quantities $\mathbf{G}'$ and $\mathbf{G}_0$ above are the physical Green function of the cluster and the noninteracting Green function of the lattice, respectively. The symbol ξ stands for a small collection of parameters that define the one-body part of H'. Tr is a functional trace, i.e., a sum over frequencies, momenta, and bands, and Ω' is the grand potential of the cluster, i.e., its ground state energy, since the chemical potential μ is included in the Hamiltonian. $\mathbf{G}'(\omega)$ and Ω' are computed numerically via the Lanczos method at zero temperature. The Potthoff functional $\Omega[\boldsymbol{\Sigma}(\xi)]$ in Eq. (3) is computed exactly, but on a restricted space of the self-energies $\boldsymbol{\Sigma}(\xi)$ that are the physical self-energies of the reference Hamiltonian H'. We use a standard optimization method (e.g., Newton-Raphson) in the space of parameters ξ to find the stationary value of $\Omega(\xi)$:

$$\frac{\partial \Omega(\xi)}{\partial \xi} = 0. \tag{4}$$

This represents the best possible value of the self-energy $\boldsymbol{\Sigma}$, which is used, together with the noninteracting Green function $\mathbf{G}_0$, to construct an approximate Green function $\mathbf{G}$ for the original lattice Hamiltonian H:

$$\mathbf{G}(\tilde{\mathbf{k}},\omega) = \frac{1}{\omega - \mathbf{t}(\tilde{\mathbf{k}}) - \boldsymbol{\Sigma}(\omega)}, \tag{5}$$

where $\tilde{\mathbf{k}}$ is a wave vector belonging to the reduced Brillouin zone, i.e., the zone associated with the superlattice of clusters, and $\mathbf{t}(\tilde{\mathbf{k}})$ is the dispersion relation. The Green function $\mathbf{G}$, along with $\mathbf{t}$, are in a mixed representation: real space up to the cluster size (hence they are matrices) and k space beyond that (hence their dependence on $\tilde{\mathbf{k}}$). The self-energy $\boldsymbol{\Sigma}(\omega)$, being limited to the cluster, does not depend on $\tilde{\mathbf{k}}$. From that Green function one can compute the average of any one-body operator, in particular the order parameters associated with magnetism. The actual value of $\Omega(\xi)$ at the stationary point is a good approximation to the physical grand potential of the lattice Hamiltonian H.

There may be more than one stationary solution to Eq. (4). For instance: A *normal state* solution in which all Weiss fields used to describe broken symmetries are zero, and another solution, with a nonzero Weiss field, describing a broken symmetry state. As an additional principle, we assert that the solution with the lowest value of the functional (3) is the physical solution [39]. Thus competing phases may be compared via their value of the grand potential Ω, obtained by introducing different Weiss fields.

III. RESULTS AND DISCUSSION

In order to probe magnetism in the Hubbard-Kondo model, we introduce the following local operators [for the conduction electrons as well as the f fermions in Eq. (2)] in the cluster Hamiltonian, within the VCA:

$$\hat{M}_{\mathbf{Q}} = M_{\mathbf{Q}} \sum_i e^{i\mathbf{Q}\cdot\mathbf{r}_i}(n_{i\uparrow} - n_{i\downarrow}), \tag{6}$$

where $\mathbf{Q} = (\pi,\pi)$ for antiferromagnetism and $(0,0)$ for ferromagnetism, and $M_{\mathbf{Q}}$ is the Weiss field, which is determined by solving Eq. (4) ($\xi = M_{\mathbf{Q}}$). We have applied the VCA with the cluster system shown in Fig. 1, and used the AFM Weiss field $M_{(\pi,\pi)}$ at half-filling and both $M_{(\pi,\pi)}$ and $M_{(0,0)}$ away from half-filling.

A. Phase diagram at half-filling

The particle-hole symmetry of the models (1) and (2) on square lattice for $t' = 0$ at half-filling implies that $\mu = U/2$. Thus, to neatly realize half-filling ($n = 1$, where n is the total number of conduction electrons per site), we set μ to $U/2$ and t' to zero. For this case, the results of the VCA computation are described below.

Figure 2 shows the AFM order parameter as a function of $J_\perp$ for several values of U, obtained by using a single variational
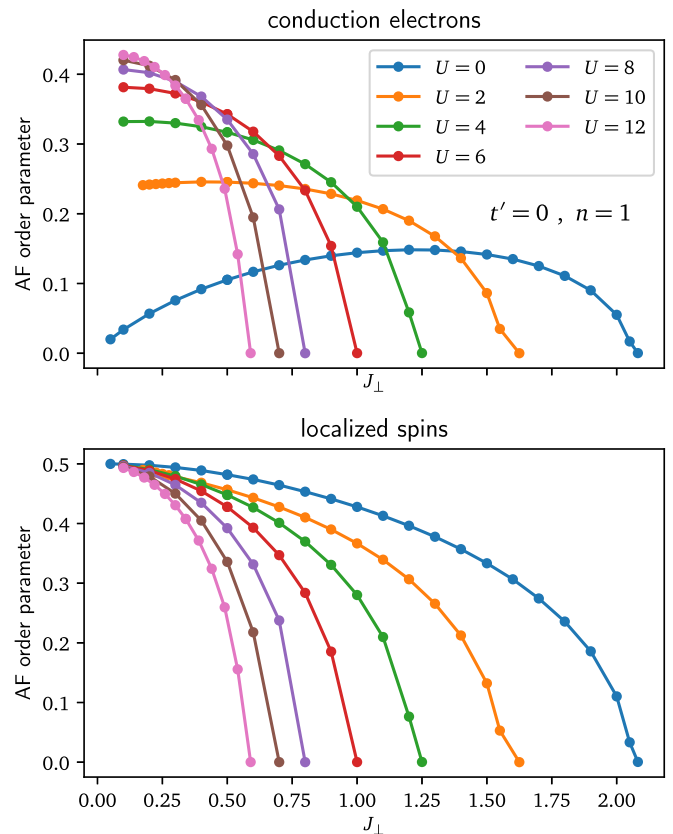
FIG. 2. The AFM order parameter of the conduction electrons (upper panel) and localized spins (lower panel) as a function of $J_\perp$ at half-filling (conduction electron density $n = 1$) for several values of the on-site repulsion U ranging from 0 to 12; from the variational cluster approximation. See text for details.
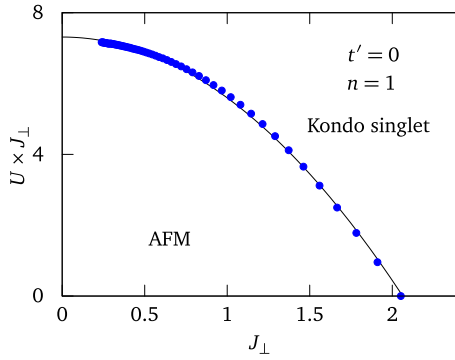
FIG. 3. Phase diagram of the Hubbard-Kondo model (2) at half-filling ($n = 1$) and $t' = 0$ in the $J_\perp$-$U J_\perp$ plane. Note how the critical U towards the Kondo singlet scales like $1/J_\perp$ when $J_\perp$ is small. The curve is a fit to the form $J_\perp(J_\perp + aU) = b$ obtained from the theory of Ref. [38], with $a \approx 0.58$ and $b \approx 4.26$.

FIG. 4. The charge gap as a function of $1/J_\perp$ at half-filling for $U = 0, 2, 4$. The second neighbor hopping t' is set to 0. The system is an insulator for any finite value of $J_\perp$.

parameter $M_{(\pi,\pi)}$ for antiferromagnetism in the conduction band. The upper panel shows the AFM order parameter for the conduction electrons and the lower panel the corresponding quantity for the localized spins. Upon increasing $J_\perp$, the system undergoes, as expected, a continuous transition from the AFM phase to the Kondo singlet phase at some critical value of $J_\perp$. This critical value decreases upon increasing U, and therefore the singlet phase is favored by the on-site repulsion between the conduction electrons. The effect of U is mainly to suppress any RKKY phase which needs itinerant electrons to mediate the magnetic interaction.

The exchange interaction alone can be responsible for both magnetic and Kondo singlet phases depending on its strength, as we can see from the $U = 0$ curve. For $U = 0$, the critical exchange interaction is found to be $J_\perp = 2.05$, quite a bit larger than the value $J_\perp = 1.45$ found using the Monte Carlo method [9]. This can be attributed to the small cluster size, which quenches the destabilizing action of spin waves, which can only act within the cluster itself. In comparison, the calculations in Ref. [38] give a slightly lower critical value of $J_\perp = 1.12$. At $U = 0$ the AFM order parameter for the conduction electrons goes to zero as $J_\perp \to 0$, but it is nonzero at $J_\perp = 0$ for any finite value of U, as known for the Hubbard model on square lattice. Notice that this is not the case for the AFM order parameter of the localized spins, which tends to a finite value as $J_\perp \to 0$ for $U = 0$.

Collecting all the critical $J_\perp$'s for different values of U in Fig. 2, we obtain the phase diagram shown in Fig. 3. The system goes from an antiferromagnet to a Kondo singlet upon increasing $J_\perp$ or U. The Hubbard interaction U favors the Kondo singlet phase, as increasing U at fixed $J_\perp$ brings the system from the AFM to the Kondo singlet phase. Overall, our phase diagram is in agreement with the one obtained using the Monte Carlo method [29]. Interestingly, the critical value of U is found to scale like $1/J_\perp$ when $J_\perp$ is small, i.e., the phase boundary tends towards a finite value of $U J_\perp$ as $J_\perp \to 0$. This being said, at $J_\perp = 0$, the system will always remain an antiferromagnet, as it will always be a Kondo singlet if $J_\perp$ is large enough. The theory of Kondo insulators of Ref. [38] provides the following leading behavior for the critical boundary between the AFM and Kondo singlet phases:
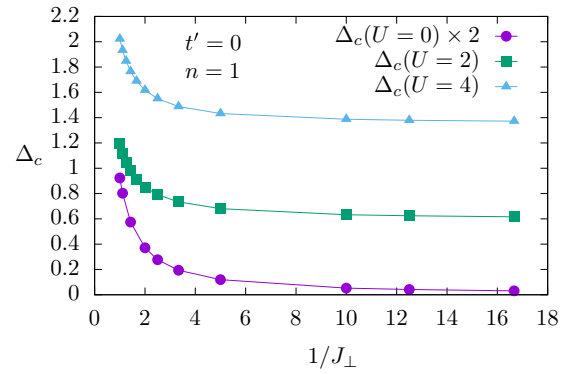
$J_\perp(J_\perp + aU) = b$, where a is a positive constant and b is a power series in $\frac{1}{(J_\perp + aU)^2}$. At leading order, b is just a positive constant, and is treated here as such. Indeed, the phase boundary in Fig. 3 looks quite like a parabola where from our numerical data $a \approx 0.58$ and $b \approx 4.26$. Notably, it also explains why U helps the Kondo singlet. It does so because it adds to $J_\perp$ and acts likewise.

Figure 4 shows the charge gap Δ_c as a function of $1/J_\perp$, for $U = 0$, 2, and 4. At a fixed U, increasing $J_\perp$ increases the spectral gap. At half-filling, the system is always an insulator for all values of $J_\perp$ and U, both in the AFM and the Kondo singlet phases. But depending on the strength of $J_\perp$ (and U), the charge gap comes from different points in the Brillouin zone [38].

In Fig. 5 we show the spectral function in the two phases at $U = 1$. In the AFM phase (top panel, $J_\perp = 0.5$), the spectral (one-particle) gap opens along the AFM zone boundary, as expected. By contrast, in the Kondo singlet phase (bottom panel, $J_\perp = 3$), the spectral gap is more or less constant across the zone and the spectrum resembles more that of a Mott insulator. This is because the charge gap in a Kondo insulator is the cost of destroying a singlet locally by adding or removing a conduction electron [40], which is exactly like the Mott gap, that is, the cost of adding or removing an electron in the half-filled Hubbard model. Notably, the approach developed by Kumar *et al.* nicely establishes the similarity between the Kondo and Mott-Hubbard insulators [38,41]. The charge gap in the half-filled Hubbard-Kondo lattice model from our VCA calculations is basically showing the same. Our VCA method does not allow access to the (two-particle) spin gap, which is expected to vanish in the AFM phase because of Goldstone's theorem.

B. Phase diagram at finite doping

We now push the system away from half-filling, going to small doping $\delta = 1 - n$ by changing the number of conduction electrons. In order to guarantee that the spin susceptibility of the host metallic state at small δ is peaked at wave vector $\mathbf{Q} = (\pi,\pi)$, we add a second-neighbor hopping, $t' = -0.3$ [42]. Note that the presence of a nonzero t' breaks particle-hole symmetry in the model, which helps bringing the system

AFM: $U = 1$, $J_\perp = 0.5$
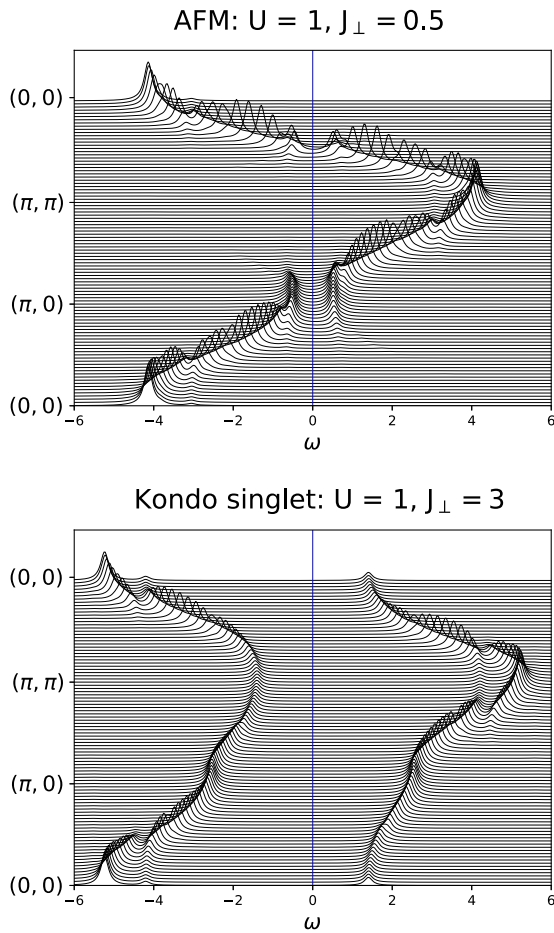
Kondo singlet: $U = 1$, $J_\perp = 3$

FIG. 5. The spectral function in the AFM (upper panel, $J_\perp = 0.5$) and in the Kondo singlet phase (lower panel, $J_\perp = 3$) at half-filling. The on-site repulsion U is set to 1 and $t' = 0$. The Fermi level is located at zero frequency and the Lorentzian broadening is set to $\eta = 0.12$.

FIG. 6. Phase diagram of the Hubbard-Kondo lattice model (2) in the ($J_\perp, \delta$) plane. At moderate $J_\perp$, the ground state is an antiferromagnet (AFM) at lower doping δ and a ferrimagnet (fM) at higher doping, before transiting towards the singlet phase. The Kondo singlet phase is stable at large $J_\perp$ for all electronic densities. The Coulomb interaction is set to $U = 2$ and $U = 4$, and the second-neighbor hopping to $t' = -0.3$.

sufficiently high values. But now, unlike the half-filled case, the transition between the Kondo singlet and magnetically ordered phases becomes discontinuous (first order). Moreover, if we compare the critical $J_\perp$'s near $\delta = 0$ in Fig. 6 with the corresponding data in Fig. 2, it is clear that a nonzero t' reduces the critical $J_\perp$ for the Kondo singlet phase.

IV. CONCLUSION

We solved the Hubbard-Kondo lattice model (of interacting conduction electrons coupled to localized spins) numerically using the variational cluster approximation method. We obtained its ground state phase diagram in the $J_\perp$-$U J_\perp$ plane at half-filling relevant to Kondo insulators, and in the δ-$J_\perp$ plane at finite dopings relevant to metallic heavy fermion systems. At half-filling, the model exhibits a continuous transition from Néel antiferromagnetism at small $J_\perp$'s to the Kondo singlet phase at large $J_\perp$'s with a critical $J_\perp$ that decreases with increasing U. The boundary between the two phases is described by the equation, $J_\perp(J_\perp + aU) = b$, for $a \approx 0.58$ and $b \approx 4.26$. Away from half-filling, the antiferromagnetic phase survives at small doping, but a ferrimagnetic phase appears at larger doping and lower $J_\perp$. The Kondo singlet phase is stable at strong $J_\perp$. The transition from the Kondo singlet to the magnetic phases becomes discontinuous at finite dopings.

smoothly away from half-filling in the variational cluster approximation. It also adds magnetic frustration to the system. The results are presented in Fig. 6 in the ($J_\perp, \delta$) plane.

Close to $\delta = 0$, the ground state remains antiferromagnetic. Upon increasing δ, the conduction electrons prefer to order ferromagnetically. The localized spins also do the same. But relative to each other, these two subsystems order antiferromagnetically. However, the net magnetization is nonzero because the conduction electron magnetization does not fully cancel the magnetization of the localized moments. Hence, we like to call this a "ferrimagnetic" (fM) phase. The critical doping where the AFM phase disappears completely is about $\delta \approx 0.09$ at $U = 2$ and $\delta \approx 0.08$ at $U = 4$. The fM phase extends to larger dopings for small $J_\perp$, since in this limit, the Kondo singlet formation gets weaker and a larger doping does not favor the AFM phase.

At any finite doping (with magnetic order at low $J_\perp$), the Kondo singlet phase is always reached by increasing $J_\perp$ to

[1] L. Childress, M. V. Gurudev Dutt, J. M. Taylor, A. S. Zibrov, F. Jelezko, J. Wrachtrup, P. R. Hemmer, and M. D. Lukin, Science **314**, 281 (2006).

[2] J. Kondo, Prog. Theor. Phys. **32**, 37 (1964).

[3] J. R. Schrieffer and P. A. Wolff, Phys. Rev. **149**, 491 (1966).

[4] P. Misra (ed.), *Heavy-Fermion Systems*, Handbook of Metal Physics, Vol. 2 (Elsevier, Amsterdam, 2008), pp. 291–333.

[5] P. Coleman, *Introduction to Many-Body Physics* (Cambridge University Press, Cambridge, 2015).

[6] M. Z. Hasan, S.-Y. Xu, and M. Neupane, Topological insulators, topological Dirac semimetals, topological crystalline insulators, and topological Kondo insulators, in *Topological Insulators, Fundamentals and Perspectives* (John Wiley and Sons, New York, 2015).

[7] F. H. L. Essler, T. Kuzmenko, and I. A. Zaliznyak, Phys. Rev. B **76**, 115108 (2007).

[8] Z.-P. Shi, R. R. P. Singh, M. P. Gelfand, and Z. Wang, Phys. Rev. B **51**, 15630 (1995).

[9] F. F. Assaad, Phys. Rev. Lett. **83**, 796 (1999).

[10] C. Jurecka and W. Brenig, Phys. Rev. B **64**, 092406 (2001).

[11] J. R. Iglesias, C. Lacroix, and B. Coqblin, Phys. Rev. B **56**, 11820 (1997).

[12] C. Lacroix and M. Cyrot, Phys. Rev. B **20**, 1969 (1979).

[13] M. N. Kiselev, D. N. Aristov, and K. Kikoin, Phys. Rev. B **71**, 092404 (2005).

[14] C. Brünger, F. F. Assaad, S. Capponi, F. Alet, D. N. Aristov, and M. N. Kiselev, Phys. Rev. Lett. **100**, 017202 (2008).

[15] D. N. Aristov, C. Brünger, F. F. Assaad, M. N. Kiselev, A. Weichselbaum, S. Capponi, and F. Alet, Phys. Rev. B **82**, 174410 (2010).

[16] S. Doniach, in *Theoretical and Experimental Aspects of Valence Fluctuations and Heavy Fermions*, edited by L. C. Gupta and S. K. Malik (Springer, Boston, MA, 1987), pp. 179–185.

[17] P. Fulde, V. Zevin, and G. Zwicknagl, Z. Phys. B **92**, 133 (1993).

[18] T. Brugger, T. Schreiner, G. Roth, P. Adelmann, and G. Czjzek, Phys. Rev. Lett. **71**, 2481 (1993).

[19] A. Furusaki and N. Nagaosa, Phys. Rev. Lett. **72**, 892 (1994).

[20] Y. M. Li, Phys. Rev. B **52**, R6979 (1995).

[21] P. Fröjdh and H. Johannesson, Phys. Rev. B **53**, 3211 (1996).

[22] T. Schork, Phys. Rev. B **53**, 5626 (1996).

[23] N. Shibata, T. Nishino, K. Ueda, and C. Ishii, Phys. Rev. B **53**, R8828 (1996).

[24] K. Itai and P. Fazekas, Phys. Rev. B **54**, R752 (1996).

[25] T. Schork and S. Blawid, Phys. Rev. B **56**, 6559 (1997).

[26] I. Hagymási, K. Itai, and J. Sólyom, Phys. Rev. B **85**, 235116 (2012).

[27] A. Georges, G. Kotliar, W. Krauth, and M. J. Rozenberg, Rev. Mod. Phys. **68**, 13 (1996).

[28] T. Pruschke, M. Jarrell, and J. Freericks, Adv. Phys. **44**, 187 (1995).

[29] M. Feldbacher, C. Jurecka, F. F. Assaad, and W. Brenig, Phys. Rev. B **66**, 045103 (2002).

[30] C. Dahnken, M. Aichhorn, W. Hanke, E. Arrigoni, and M. Potthoff, Phys. Rev. B **70**, 245110 (2004).

[31] M. Potthoff, in *Theoretical methods for Strongly Correlated Systems*, Springer Series in Solid-State Sciences, Vol. 171, edited by A. Avella and F. Mancini (Springer, New York, 2012), Chap. 9.

[32] M. Potthoff, in *DMFT at 25: Infinite dimensions, Lecture Notes of the Autumn School on Correlated Electrons 2014*, edited by E. Pavarini, E. Koch, D. Vollhardt, and A. Lichtenstein (Forschungszentrum, Jülich, 2014).

[33] Q. Si and F. Steglich, Science **329**, 1161 (2010).

[34] D. Sénéchal, P.-L. Lavertu, M.-A. Marois, and A.-M. S. Tremblay, Phys. Rev. Lett. **94**, 156404 (2005).

[35] M. Aichhorn, E. Arrigoni, M. Potthoff, and W. Hanke, Phys. Rev. B **74**, 235117 (2006).

[36] A. H. Nevidomskyy, C. Scheiber, D. Sénéchal, and A.-M. S. Tremblay, Phys. Rev. B **77**, 064427 (2008).

[37] M. Potthoff, Eur. Phys. J. B **32**, 429 (2003).

[38] P. Ram and B. Kumar, Phys. Rev. B **96**, 075115 (2017).

[39] M. Potthoff, AIP Conf. Proc. **816**, 41 (2006).

[40] This is different from the spin gap in Kondo insulators, which is the cost of creating a triplet excitation.

[41] B. Kumar, Phys. Rev. B **77**, 205115 (2008).

[42] L. C. Martin, M. Bercx, and F. F. Assaad, Phys. Rev. B **82**, 245105 (2010).